Contents lists available at SciVerse ScienceDirect

Comptes Rendus Chimie

www.sciencedirect.com

Preliminary communication/Communication

First nanoparticles of Bechgaard salts

Dominique de Caro [a,b,*], Kane Jacob [a,b], Christophe Faulmann [a,b], Lydie Valade [a,b]

[a] CNRS, Laboratoire de Chimie de Coordination (LCC), 205, route de Narbonne, BP 44099, 31077 Toulouse cedex 4, France
[b] Université de Toulouse, UPS, INPT, 31077 Toulouse cedex 4, France

ABSTRACT

Well-dispersed nanoparticles of the superconducting Bechgaard salts, namely $(TMTSF)_2PF_6$ and $(TMTSF)_2ClO_4$, have been electrochemically grown in organic solution in the presence of a supporting electrolyte either being an ionic liquid or a long alkyl-chains quaternary ammonium salt. Nanoparticles exhibit sizes in the 20–75 nm range. Nanoparticle powders have been characterized by infrared, Raman, visible absorption spectroscopy, and by preliminary transport measurements at room temperature.

© 2013 Académie des sciences. Published by Elsevier Masson SAS. All rights reserved.

RÉSUMÉ

Des nanoparticules de supraconducteurs moléculaires, couramment désignés par le terme « sels de Bechgaard », ici $(TMTSF)_2PF_6$ et $(TMTSF)_2ClO_4$, ont été obtenues par voie électrolytique dans un solvant organique en présence d'un électrolyte support de type liquide ionique ou sel d'ammonium quaternaire présentant plusieurs longues chaînes alkyles. Une étude par microscopie électronique à transmission met en évidence des nanoparticules de taille comprise entre 20 et 75 nm. Les poudres nanoparticulaires ainsi préparées ont été caractérisées par spectrométrie infrarouge et Raman, par spectroscopie d'absorption dans le visible, mais également par des mesures préliminaires de conductivité à température ambiante.

© 2013 Académie des sciences. Publié par Elsevier Masson SAS. Tous droits réservés.

1. Introduction

Organic superconductors prepared as single crystals have attracted much attention in the 1980–1990s [1]. For instance, the so-called Bechgaard salts, $(TMTSF)_2X$, have been prepared by electro-oxidation of tetramethyltetra-selenafulvalene (TMTSF, Fig. 1) in the presence of an electrolyte, such as $[(n\text{-}C_4H_9)_4N]X$, where X stands for a monovalent inorganic anion (X^-: PF_6^-, AsF_6^-, ClO_4^-, ReO_4^-).

Under high current densities ($> 60\ \mu A/cm^2$), needle-shaped crystals of $(TMTSF)_2ClO_4$ have been obtained (typical sizes: $10\text{–}30 \times 0.5\text{–}2 \times 0.1\text{–}1\ mm^3$) [2,3]. Since the 2000s, a new interest has emerged due to the fact that these compounds have been prepared in a more practical usable form, such as thin films or microwires. As an example, $(TMTSF)_2ClO_4$ has been grown as microcrystals in a confined environment [4], as thin layers on an organic template [5], as thin films on a (001)-oriented silicon substrate [6], or as micro/nanowires [7].

However, at present, spherical nanoparticles of mole-cule-based conductors are very rare. Indeed, the spherical shape constitutes a "challenging" morphology for com-pounds, which naturally grow as needles, or wires due to
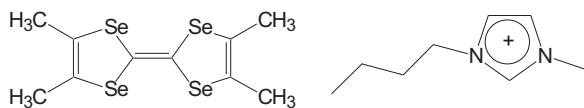
Fig. 1. Molecular formulas for TMTSF and 1-butyl-3-methylimidazolium.

their quasi-one-dimensional character. We have recently obtained roughly spherical nanoparticles of tetrathiafulvalene (TTF)-based conductors protected by a polymer matrix [8], or grown in the presence of an ionic liquid or a long alkyl-chains quaternary ammonium salt [9–11]. In this present communication, we report on the preparation of the first nanoparticles of two Bechgaard salts, namely $(TMTSF)_2PF_6$ and $(TMTSF)_2ClO_4$.

2. Results and discussion

$(TMTSF)_2X$ phases behave as good organic metals with a room temperature conductivity of about 600 S/cm at 300 K (measured along the needle axis). Single crystals of $(TMTSF)_2PF_6$ become superconducting at pressures above 6 kbar (critical temperature in the $0.9 - 1.2$ K range) whereas those of $(TMTSF)_2ClO_4$ are superconducting at ambient pressure (critical temperature between 1.2 and 1.4 K) [1]. As mentioned in the introduction, millimeter-sized single crystals of $(TMTSF)_2X$ are grown in an electrochemical cell containing a tetrabutylammonium salt acting as both supporting electrolyte and provider of the X^- ion. The absence of stirring is required to get high quality large single crystals for performing structural studies. Ionic liquids containing a 1,3-dialkylimidazolium cation (such as, 1-butyl-3-methylimidazolium $BMIM^+$, Fig. 1) or long alkyl-chains quaternary ammonium salts (such as, $[(CH_3)(n\text{-}C_8H_{17})_3N]Cl$) in addition to a polar solvent (acetonitrile, acetone) allow the preparation of nanoparticles of $TTFCl_{0.77}$ [12], TTF·TCNQ [10], or TTF[Ni(dmit)$_2$]$_2$ [11]. In the case of electrochemically grown $TTFCl_{0.77}$ nanoparticles [12], the ammonium salt plays a triple role: supporting electrolyte, provider of the chlorine counter ion, and entity allowing the control of the growth of the conducting material as nanospheres at the electrode surface.

In this work, we have performed the galvanostatic oxidation ($\sim 30 \, \mu A/cm^2$) of TMTSF in the presence of the ionic liquid, $[BMIM][PF_6]$, or of the long alkyl-chains quaternary ammonium salt, $[(CH_3)(n\text{-}C_8H_{17})_3N]ClO_4$, as the supporting electrolyte under vigorous stirring. A black solid is obtained on the platinum electrode located in the anodic compartment. Vibrational spectra (infrared and Raman, vide infra) confirm that the powder corresponds to $(TMTSF)_2PF_6$ when the electrochemical reaction is performed in the presence of $[BMIM][PF_6]$, whereas it corresponds to $(TMTSF)_2ClO_4$ when the electrochemical reaction is carried out in the presence of $[(CH_3)(n\text{-}C_8H_{17})_3N]ClO_4$. Infrared and Raman spectra are shown on Figs. 2 and 3, and the corresponding data are gathered in Table 1. The two Raman spectra are very similar and only that for the $(TMTSF)_2ClO_4$ powder is shown. Signals are assigned according to references [13–15]. Low intensity features on infrared spectra (in the $3000 - 1300 \, cm^{-1}$
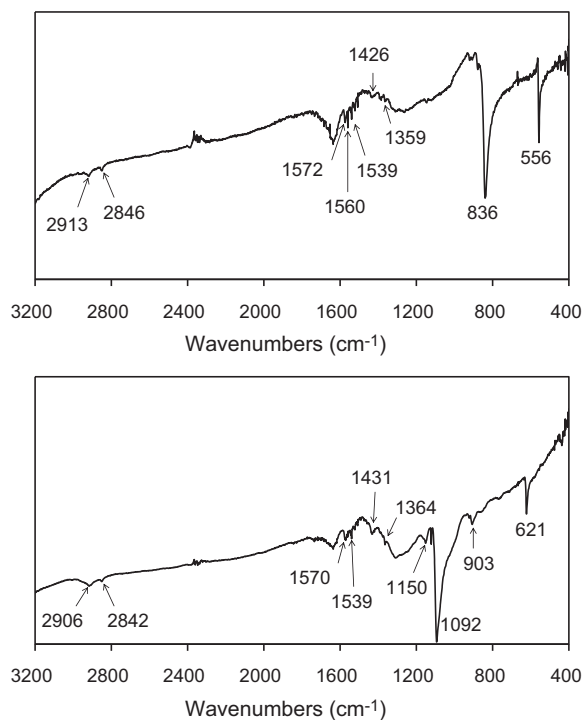

Fig. 2. Infrared spectra for $(TMTSF)_2PF_6$ (top) and $(TMTSF)_2ClO_4$ (bottom) nanoparticles.

range) are mainly due to the TMTSF molecule (Table 1). C–H stretching modes of the methyl groups are located in the $2920–2840 \, cm^{-1}$ region. These signals confirm unambiguously the presence of the TMTSF moiety within the electrochemically grown powders. Medium and strong intensity signals at lower frequencies are characteristic of the counter ion. Modes for the hexafluorophosphate anion are located at 836 and $556 \, cm^{-1}$, whereas those for the perchlorate anion are located at 1092 and $621 \, cm^{-1}$. Low-frequency Raman peaks (in the $100–1000 \, cm^{-1}$ range) are attributed by the comparison to those for neutral TMTSF [14]. Their positions are not too much affected by the partial charge-borne by the TMTSF molecule. On the contrary, modes assigned to the C=C stretches (in the $1450–1600 \, cm^{-1}$ range) display a large shift by comparison to the neutral TMTSF molecule [14,15]. The
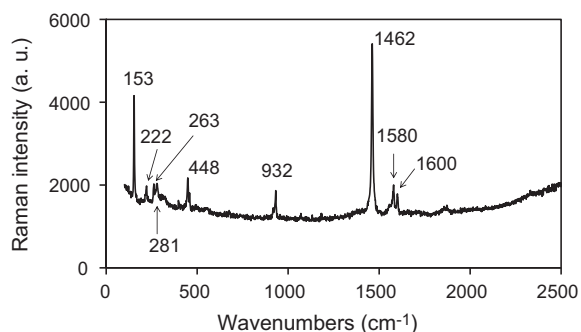

Fig. 3. Raman spectrum for $(TMTSF)_2ClO_4$ nanoparticles.

Table 1

Spectral data for nanoparticles of $(TMTSF)_2PF_6$ and $(TMTSF)_2ClO_4$.

	$(TMTSF)_2PF_6$	$(TMTSF)_2ClO_4$	Assignment
Infrared spectra, frequencies (cm^{-1})	2913	2906	νCH_3 asym.
	2846	2842	νCH_3 sym.
	1572	1570	$\nu C=C$ (ν_{28}, b_{1u})
	1539	1539	$\nu C=C$
	1426	1431	$\alpha\ CH_3$ asym.
	1359	1364	$\alpha\ CH_3$ sym.
	–	1092	ClO_4^-
	836	–	PF_6^-
	–	621	ClO_4^-
	556	–	PF_6^-
Raman spectra, frequencies (cm^{-1})	1601	1600	Peripherical C=C stretch (ν_3, a_g)
	1580	1580	
	1460	1462	Central C=C stretch (ν_4, a_g)
	931	932	$\beta\ CH_3$
	448	448	ν_9, a_g
	278	281	ν_{10}, a_g
	262	263	ν_{11}, a_g
	153	153	ν_{12}, a_g
Absorption spectra, wavelenghts in nm (in brackets, cm^{-1})	773 (12,900)	776 (12,900)	Intramolecular excitations of TMTSF
	585 (17,100)	589 (17,100)	
	451 + shoulder at 429 (22,200 + sh. at 23,300)	451 + shoulder at 431 (22,200 + sh. at 23,300)	
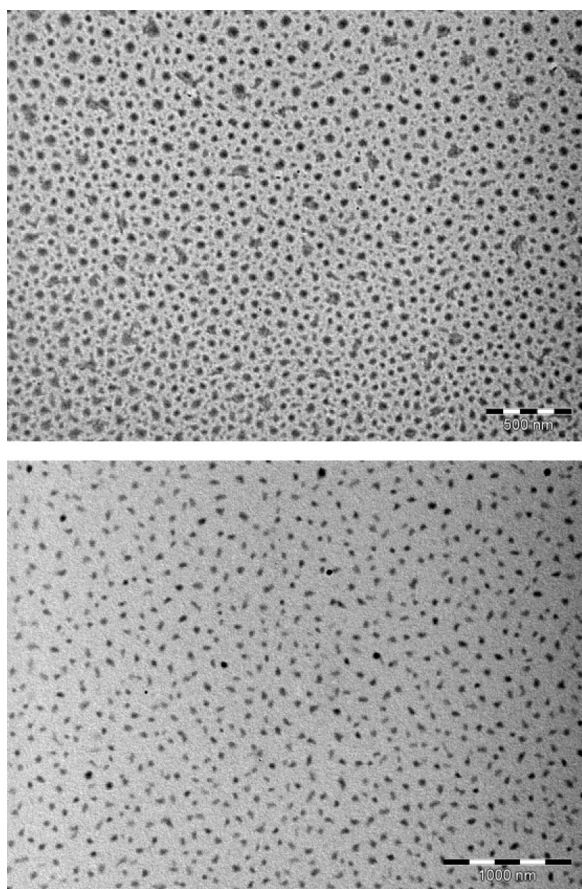
Fig. 4. Electron micrographs for $(TMTSF)_2PF_6$ (top, bar = 500 nm) and $(TMTSF)_2ClO_4$ (bottom, bar = 1000 nm) nanoparticles.

position of the more intense signal ($\sim 1460\ cm^{-1}$) is in good agreement with a 0.5 formal charge-borne by the TMTSF moiety [15], thus, confirming the 2 $TMTSF^{0.5+}$/1 PF_6^- or ClO_4^- stoichiometry within the powders. For the $(TMTSF)_2PF_6$ powder, electron micrographs evidence a majority of roughly spherical nanoparticles, exhibiting diameters in the 20–60 nm range, in addition with some bigger particles (60–75 nm), showing irregular shapes (Fig. 4). For the $(TMTSF)_2ClO_4$ powder, nanoparticles exhibit sizes in the 30–75 nm range, most of them being elongated in shape. Thus, the galvanostatic oxidation of the TMTSF molecule dissolved in a mixture of the ionic liquid, [BMIM][PF_6], or of the long alkyl-chains quaternary ammonium salt, [$(CH_3)(n$-$C_8H_{17})_3$N]ClO_4, and CH_2Cl_2 provides nanoparticle powders of either $(TMTSF)_2PF_6$, or $(TMTSF)_2ClO_4$. The literature reports on the preparation of needle-shaped single crystals of $(TMTSF)_2NbF_6$ by electro-oxidation of TMTSF dissolved in a mixture of [EMIM][NbF_6] (E for ethyl) and CH_2Cl_2 [16]. In our case, stirring the medium presumably prevent the formation of large single crystals. It also increases the concentration of ionic liquid at the electrode vicinity and favours the growth control of the material as nanoparticles. Moreover, in our case, the use of an imidazolium cation bearing a longer alkyl chain (butyl vs ethyl) is an additional argument to the formation of nanoparticles, as previously reported [9–11]. Furthermore, as stated above, the electro-oxidation of tetrathiafulvalene in the presence of [$(CH_3)(n$-$C_8H_{17})_3$N]Cl affords nanoparticles of $TTFCl_{0.77}$ [12]. Hence, in the present work, the formation of $(TMTSF)_2ClO_4$ as a nanoparticle powder when the electrochemical synthesis is conducted with [$(CH_3)(n$-$C_8H_{17})_3$N]ClO_4 is also easily understandable. We can conclude that in a vigorously stirred electrochemical cell, [BMIM][PF_6] or [$(CH_3)(n$-$C_8H_{17})_3$N]ClO_4 act as the supporting electrolyte, the entity that control the growth as nanoparticles, and the provider of the PF_6^- or

ClO_4^- anion necessary for the formation of the molecule-based superconductors, i.e., $(TMTSF)_2PF_6$, and $(TMTSF)_2ClO_4$. $(TMTSF)_2X$ ($X = PF_6$, ClO_4) nanopowders are soluble in acetonitrile (about 2.5 mg/mL) and insoluble in toluene, hexane, ethanol, tetrahydrofurane, dichloromethane and 1,1,2-trichloroethane. After air exposure (~ 2 h) and acetonitrile evaporation, infrared spectra and transmission electron micrographs of the solid residue do not exhibit significant changes compared to those of freshly electrodeposited powders. Note that at room temperature, powdered bulk $(TMTSF)_2PF_6$ and $(TMTSF)_2ClO_4$ have been shown to be soluble in 1,1,2- and 1,1,1-trichloroethane (about 0.2 mg/mL), whereas they are negligibly soluble in tetrahydrofurane or in a toluene/ethanol mixture [17]. Moreover, needle-like $(TMTSF)_2ClO_4$ single crystals have been dissolved in acetonitrile at ambient temperature, a further small heating accelerating their solubility [7a]. Therefore, the solubility of our $(TMTSF)_2X$ nanopowders in acetonitrile was expected. Furthermore, the good solubility observed for $(TMTSF)_2X$ nanopowders in acetonitrile is consistent with that for tetrathiafulvalene- or nickel ethylene tetrathiolate-based conductors as nanoparticles (grown in the presence of a long alkyl chain amine or imidazolium salt), which are very soluble in commonly used polar solvents (tetrahydrofurane, methanol, acetonitrile; 2–5 mg/mL) [18]. Absorption spectra for $(TMTSF)_2PF_6$ and $(TMTSF)_2ClO_4$ in acetonitrile are almost identical (Table 1), and only that for $(TMTSF)_2PF_6$ is shown (Fig. 5). It evidences maxima at 773 nm (~ 12900 cm^{-1}, strong), 585 nm (~ 17100 cm^{-1}, weak), and 451 nm (~ 22200 cm^{-1}, strong). They correspond to intramolecular transitions of the cationic TMTSF moiety [19]. These three characteristic absorptions appear at similar positions for numerous organic conductors [19]. For instance, they are located at ~ 13500 cm^{-1} (strong), ~ 18400 cm^{-1} (weak), and ~ 22400 cm^{-1} (strong) for $(BPDT-TTF)_3(PF_6)_2$ (BPDT: bis(propylenedithio)tetrathiafulvalene) [20]. Finally, preliminary room temperature conductivity measurements on nanoparticle powders give values of about 0.2 S/cm, of the same order of magnitude than those for bulk powder materials. This bodes that, in the powder, which is actually made of nanoparticles, conduction paths do also exist. For further applications, more interesting would be the deposition of these $(TMTSF)_2X$-based nano-objects onto

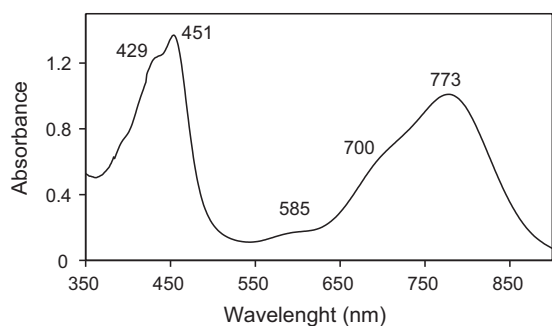predefined nanoscale regions of a silicon chip [21]. This study will be soon envisioned. In conclusion, by using a judicious supporting electrolyte, we have prepared the first nanoparticles of the well-known Bechgaard salts. They exhibit sizes in the 20–75 nm range. We are currently investigating the use of different experimental conditions (temperature of the electrochemical growth, potentiostatic conditions) and the addition of a neutral surfactant to the electrolyte solution. Indeed, these latter allow the preparation of very small particles of spin crossover compounds [22]. The preparation of much smaller nanoparticles (≤ 5 nm) than those described in this communication constitutes a challenge for us. This should allow the emergence of a new physics for nano-molecular superconductors, as the recent study of superconductivity in few pairs of $(BETS)_2GaCl_4$ (BETS: bis(ethylenedithio)tetraselenafulvalene) molecules on an Ag(111) surface [23].

3. Experimental

Electrochemical syntheses have been carried out under an argon atmosphere using freshly distilled and degassed dichloromethane. TMTSF is purchased from Aldrich and [BMIM][PF_6] from Alfa Aesar. [$(CH_3)(n-C_8H_{17})_3$N]ClO_4 is prepared as follows: a solution of 160 mg of $LiClO_4$ (1.50 mmol) in 5 mL water is slowly added to a solution of 430 mg of [$(CH_3)(n-C_8H_{17})_3$N]Cl (1.07 mmol) in 15 mL of water. The resulting solution is then stirred for 18 h at room temperature. [$(CH_3)(n-C_8H_{17})_3$N]ClO_4 is extracted by dicholoromethane, dried on $MgSO_4$, and finally, recrystallized from a dicholoromethane/pentane mixture.

A typical electrochemical procedure can be described as follows: nanoparticles synthesis takes place in an H-shaped electrocrystallization cell with a platinum wire (1 cm long; 1 mm diameter) in each compartment, separated by a glass frit in the H cross piece. TMTSF (25 mg; 0.056 mmol), [BMIM][PF_6] (80 mg; 0.28 mmol) [or [$(CH_3)(n-C_8H_{17})_3$N]ClO_4 (130 mg; 0.28 mmol)] and 12 mL dicholoromethane are introduced in the anodic compartment. The same amount of [BMIM][PF_6] (i.e. 80 mg; 0.28 mmol) [or [$(CH_3)(n-C_8H_{17})_3$N]ClO_4 (i.e. 130 mg; 0.28 mmol)] and 12 mL dicholoromethane are introduced in the cathodic compartment, leading to a total molar ratio [BMIM][PF_6]/TMTSF [or [$(CH_3)(n-C_8H_{17})_3$N]ClO_4/TMTSF] of about 10. The synthesis is conducted under galvanostatic conditions (30 μA/cm^2) at room temperature in argon atmosphere during 6 days for $(TMTSF)_2PF_6$ [or 3 days for $(TMTSF)_2ClO_4$]. During the electrochemical synthesis, the content of the cell is vigorously agitated with a magnetic stirrer. The black powder is collected from the anode, washed with 2×1.5 mL dichloromethane, and finally dried under vacuum for 24 h (yield: 60% for $(TMTSF)_2PF_6$ and 90% for $(TMTSF)_2ClO_4$). The black powder is air stable.

The room temperature solubility of the nanopowdered samples in organic solvents is evaluated by the stepwise addition of a determined volume of solvent to the powder under slow stirring (organic solvents: acetonitrile, toluene, hexane, ethanol, tetrahydrofurane, dichloromethane, and 1,1,2-trichloroethane). For transmission electron microscopy observation, powder (0.5 mg) is dispersed in diethyl ether (2 mL) under slow stirring for 1 min. The TEM

Fig. 5. Absorption spectrum for $(TMTSF)_2PF_6$ nanoparticles.

specimens are then prepared by the evaporation of droplets of suspension deposited on carbon-supported copper grids. The experiments are performed on a JEOL Model JEM 1011 operating at 100 kV. Infrared spectra (in KBr matrix) are taken at room temperature on a Perkin Elmer Spectrum GX spectrophotometer. Raman spectra are recorded on the powder sample at 80 K using a DILOR XY micro-Raman (785 nm laser line). Absorption spectra are taken in the 350–900 nm range on a Perkin Elmer Lambda 35 spectrophotometer ($\sim$ 3 mmol/L in acetonitrile). The room temperature conductivity of the samples is measured on a compressed pellet by two-probe contacts.

References

[1] (a) T. Ishiguro, K. Yamaji, G. Saito (Eds.), Organic Superconductors, second ed., Springer-Verlag, Berlin Heidelberg, New York, 1998;
(b) D. Jérome, in : A.G. Lebed (Ed.), The Physics of Organic Superconductors and Conductors, Springer-Verlag, Berlin Heidelberg, 2008, p. 3;
(c) S.E. Brown, P.M. Chaikin, M.J. Naughton, in : A.G. Lebed (Ed.), The Physics of Organic Superconductors and Conductors, Berlin Heidelberg, 2008, p. 49.

[2] K. Bechgaard, C.S. Jacobsen, K. Mortensen, H.J. Pedersen, N. Thorup, Solid State Commun. 33 (1980) 1119.

[3] K. Bechgaard, K. Carneiro, F.B. Rasmussen, M. Olsen, J. Am. Chem. Soc. 103 (1981) 2440.

[4] S. Perruchas, J. Fraxedas, E. Canadell, P. Auban-Senzier, P. Batail, Adv. Mater. 17 (2005) 209.

[5] A. Moradpour, M. Ribault, P. Auban-Senzier, Adv. Mater. 12 (2000) 719.

[6] J.P. Savy, D. de Caro, L. Valade, J.C. Coiffic, E.S. Choi, J.S. Brooks, J. Fraxedas, Synth. Met. 160 (2010) 855.

[7] (a) C. Colin, C.R. Pasquier, P. Auban-Senzier, F. Restagno, S. Baudron, P. Batail, J. Fraxedas, Synth. Met. 146 (2004) 273;
(b) Y.J. Jung, Y. Kim, G.T. Kim, W. Kang, D.Y. Noh, J. Nanosci. Nanotechnol. 12 (2012) 5397.

[8] M. Souque, D. de Caro, L. Valade, Synth. Met. 161 (2011) 1001.

[9] D. de Caro, K. Jacob, C. Faulmann, J.P. Legos, F. Senocq, J. Fraxedas, L. Valade, Synth. Met. 160 (2010) 1223.

[10] D. de Caro, K. Jacob, H. Hahioui, C. Faulmann, L. Valade, T. Kadoya, T. Mori, J. Fraxedas, L. Viau, New J. Chem. 35 (2011) 1315.

[11] D. de Caro, K. Jacob, C. Faulmann, L. Valade, L. Viau, C. R. Chimie 15 (2012) 950.

[12] D. de Caro, K. Jacob, S. Mazzi, M.T. Carayon, C. Faulmann, L. Valade, Synth. Met. 162 (2012) 805.

[13] R. Bozio, C. Pecile, K. Bechgaard, F. Wudl, D. Nalewajek, Solid State Commun. 41 (1982) 905.

[14] M. Meneghetti, R. Bozio, I. Zanon, C. Pecile, C. Ricotta, M. Zanetti, J. Chem. Phys. 80 (1984) 6210.

[15] R. Bozio, C. Pecile, J.C. Scott, E.M. Engler, Mol. Cryst. Liq. Cryst. 119 (1985) 211.

[16] M. Sakata, Y. Yoshida, M. Maesato, G. Saito, K. Matsumoto, R. Hagiwara, Mol. Cryst. Liq. Cryst. 452 (2006) 103.

[17] A. Angelova, A. Moradpour, P. Auban-Senzier, Synth. Met. 143 (2004) 187.

[18] (a) M. Souque, O. Vendier, L. Valade, D. de Caro, J.-M. Desmarres, F. Courtade, Patent FR 2957460, WO 2011110653, 2011. ;
(b) C. Faulmann, J. Chahine, K. Jacob, Y. Coppel, L. Valade, D. de Caro, J. Nanopart. Res. 15 (2013) 1586.

[19] A. Graja, Spectroscopy of Materials for Molecular Electronics, Scientific Publishers, Poznan, 1997.

[20] K. Yakushi, H. Tajima, T. Ida, M. Tamura, H. Hayashi, H. Kuroda, A. Kobayashi, H. Kobayashi, R. Kato, Synth. Met 24 (1988) 301.

[21] N.S. Losilla, N.S. Oxtoby, J. Martinez, F. Garcia, R. Garcia, M. Mas-Torrent, J. Veciana, C. Rovira, Nanotechnology 19 (2008) 455308.

[22] I.A. Gural'skiy, C.M. Quintero, G. Molnár, I.O. Fritsky, L. Salmon, A. Bousseksou, Chem. Eur. J. 18 (2012) 9946.

[23] K. Clark, A. Hassanien, S. Khan, K.F. Braun, H. Tanaka, S.W. Hla, Nat. Nanotechnol. 5 (2010) 261.